

The Multiplicity of the Hyades and its Implications for Binary Star Formation and Evolution

J. Patience¹, A. M. Ghez^{1,2,3}, I. N. Reid⁴,
A. J. Weinberger⁴, & K. Matthews⁴

To appear in the *Astronomical Journal*, May 1998

¹UCLA Division of Astronomy and Astrophysics, Los Angeles, CA 90095-1562

²Sloan Fellow

³Packard Fellow

⁴Palomar Observatory, California Institute of Technology, Pasadena, CA 91125

ABSTRACT

A 2.2 μm speckle imaging survey of 167 bright ($K < 8.5$ mag) Hyades members reveals a total of 33 binaries with separations spanning $0''.044$ to $1''.34$ and magnitude differences as large as 5.5 mag. Of these binaries, 13 are new detections and an additional 17 are now spatially resolved spectroscopic binaries, providing a sample from which dynamical masses and distances can be obtained. The closest 3 systems, marginally resolved at Palomar, were re-observed with the 10m Keck telescope in order to determine accurate binary star parameters. Combining the results of this survey with previous radial velocity, optical speckle, and direct imaging Hyades surveys, the detected multiplicity of the sample is: 98 singles, 59 binaries, and 10 triples.

A statistical analysis of this sample investigates a variety of multiple star formation and evolution theories. Over the binary separation range $0''.1$ to $1''.07$ (5 to 50 AU), the sensitivity to companion stars is relatively uniform, with $\langle \Delta K_{lim} \rangle = 4$ mag, equivalent to a mass ratio $\langle q_{min} \rangle = 0.23$. Accounting for the inability to detect high flux ratio binaries results in an implied companion star fraction (csf) of 0.30 ± 0.06 in this separation range. The Hyades csf is intermediate between the values derived from observations of T Tauri stars ($csf_{TTauri} = 0.40 \pm 0.08$) and solar neighborhood G-dwarfs ($csf_{SN} = 0.14 \pm 0.03$). This result allows for an evolution of the csf from an initially high value for the pre-main sequence to that found for main sequence stars.

Within the Hyades, the csf and the mass ratio distribution provide observational tests of binary formation mechanisms. The csf is independent of the radial distance from the cluster center and the primary star mass. The distribution of mass ratios is best fit by a power law $q^{-1.3 \pm 0.3}$ and shows no dependence on the primary mass, binary separation, or the radial distance from the cluster center. Overall, the Hyades data are consistent with scale-free fragmentation, but inconsistent with capture in small clusters and disk-assisted capture in small clusters. Without testable predictions, scale-dependent fragmentation and disk fragmentation cannot be assessed with the Hyades data.

1. Introduction

Early surveys of solar neighborhood stars found that binaries outnumber solitary stars (Abt & Levy 1976), and more recent results have reinforced the observation that multiples are very common (Duquennoy & Mayor 1991). Surveys of T Tauri stars, young objects only a few million years old, revealed a surprisingly large fraction of binary stars, with twice as many companions compared to solar neighborhood G-dwarfs over a semi-major axis range from ~ 10 to 250 AU (Ghez, Neugebauer & Matthews 1993; Leinert et al. 1993; Simon et al. 1995; Ghez et al. 1997). This discrepancy suggests the possibility of a decline in the overall binary frequency with time. Since the Hyades has an age ($\sim 6 \times 10^8$ yr) between the T Tauri stars and the solar neighborhood, and also has a nearby distance ($D = 46.3$ pc, Perryman et al. 1997) and carefully determined membership, the cluster is well-suited for an investigation of the evolution of the companion star fraction.

Young clusters are also ideal laboratories for binary star formation studies since they provide a sample of stars with relatively constant age, metallicity, and distance. Binary star formation models fall into two broad categories: capture and fragmentation (cf. Clarke 1996). Capture has been postulated to proceed in small-N (4-10 member) clusters either with or without the dissipative effects of disk interactions (McDonald & Clarke 1993, 1995). The restriction to small-N clusters rather than large clusters is necessary because the probability of an interaction that forms a binary is too low in large clusters (Clarke). Alternatively, different models of fragmentation have also been proposed – fragmentation of the protostellar cloud core or of the circumstellar disk (cf. Boss & Myhill 1995; Myhill & Kaula 1992; Burkert & Bodenheimer 1996; Bonnell & Bate 1994). Observable properties of binary stars, such as the distribution of mass ratios and the dependence of the companion star fraction on the primary star mass, provide important tests of binary star formation scenarios.

In this paper, the results of a speckle imaging survey of the Hyades are presented. The separation range covered, $0''.10$ to $1''.07$ (5 to 50 AU), not only fills the gap between spectroscopy and direct imaging, but also overlaps the ~ 30 AU peak of the distribution of semi-major axes measured for binary stars (Duquennoy & Mayor 1991; Mathieu 1994). The main goal of the project is to conduct a statistical analysis of the properties of the observed binary stars in order to test the predictions made by binary star formation and evolution scenarios. The membership and magnitude criteria used to select the sample are explained in §2. Section 3 describes the observations, followed by the details of the data analysis procedures presented in §4. The results of the survey and the bounds of the completeness region are given in §5, which also includes a comparison of the present survey with the considerable amount of previous work on the Hyades. In the discussion, §6, the observed

binary star properties are analyzed in order to explore theories of binary star formation and evolution. Finally, the main conclusions are summarized in §7.

2. Hyades Sample

The stars selected for this speckle survey satisfy both a magnitude limit of $K < 8.5$ mag and a membership requirement based on proper motion and photometry. The number of stars satisfying the membership and magnitude criteria is 197, and 167 of these stars were observed; the observed sample is listed in Table 1. The four red giant stars and the evolved A star in the Hyades were observed and the results are reported, but the majority of the statistical analysis is confined to the main-sequence stars. This speckle sample represents approximately one-third of the total cluster census. The target list of Hyades members was culled from the appendix of Reid (1993) which identifies probable members on the basis of proper motions and optical photometry. Because only the brighter members of the cluster are included in the speckle survey sample, most of the astrometric and photometric observations are from either the original investigation of the structure and motion of the Hyades by van Bueren (1952) or from the subsequent Leiden photographic survey by Pels et al. (1975).

Candidates identified in these early studies have been subjected to more recent and more selective membership tests with highly accurate proper motions (Schwann 1991), photometry (Mermilliod 1976), and astrometry (Perryman et al. 1997). The Hipparcos satellite measured the parallax to 139 Hyades stars in the speckle survey. Combining the results of the parallax measurements of many Hyades members provides the most accurate distance to the cluster center, 46.3 pc (Perryman). The individual proper motions, however, have a smaller uncertainty (~ 2 , % Schwann) than the individual Hipparcos parallaxes (~ 10 , % Perryman et al.). The smaller uncertainties make the proper motion data more sensitive to the relative distance between members. Because of these considerations, the distance to each star listed in Table 1 is determined by scaling the value given in Schwann (1991) by 0.966, the ratio of the distance to the cluster center measured by Hipparcos and proper motions. The distances for 25 of the faintest stars not measured by Schwann were scaled from the appendix in Reid (1993) which lists the result from the Pels et al. study.

Although optical photometry has been obtained from previous membership studies, K-band photometry is not available for most of these stars. An estimate of the K magnitude of each star was obtained by combining the V magnitude and B-V color listed in Reid (1993) with an empirical color-color transform described in the Appendix. At the 46.3 pc mean distance to the Hyades, the limiting magnitude corresponds to a minimum target star

mass of $0.46 M_{\odot}$, based on the mass- M_K relation also given in the Appendix. The depth of the cluster, 15%, causes a variation of at most $0.05 M_{\odot}$ in the target mass limit.

3. Observations

Speckle observations of the Hyades stars were obtained at a wavelength of $2.2 \mu m$ between 1993 and 1996 at the Cassegrain focus of the Hale 5 m telescope with the facility near-infrared camera. Over the three-year period that the observations were made, this instrument was upgraded; the camera array was replaced once and the reimaging optics which determine the pixel scale were changed twice. Table 2 summarizes the details of each observing run. Each night approximately twenty stars were observed, and during the last two nights, 26 stars with an initial $\Delta K_{lim} < 3.0$ (cf. §4) were reobserved to improve the data quality. Additionally, the 3 marginally-resolved binaries (vB 91, vB 96, and +10 568) were reobserved on 1996 December 22 and 1997 December 14 with the W. M. Keck 10 m telescope and its speckle imaging system (Matthews et al. 1996).

For each target star, a total of 3,000 to 4,000 exposures of ~ 0.1 seconds were recorded. These source observations were interleaved with similar observations of a reference point source in sets of ~ 500 images. The short exposure time is necessary to “freeze” the turbulent structure of the atmosphere, and a large number of images provides many samples of the instantaneous effects of the atmosphere, as required for speckle imaging. The rapid exposure permitted the use of the broad band K-filter ($\Delta\lambda = 0.4\mu m$) for most of the observations, however, six of the brightest stars – vB 28, vB 41, vB 70, vB 71, vB 8, and vB 33 – were observed through a one-percent cvf filter centered on a wavelength of $2.2 \mu m$ in order to prevent the array from saturating. Since the central wavelength of the cvf filter is identical to that of the K-band, the resolution of these six observations is comparable to that of the other stars in the sample. During one night, poor seeing conditions allowed similarly bright sources to be observed through the K-filter.

4. Data Analysis

The initial data reduction steps follow standard image analysis – the raw speckle images are sky subtracted, flat fielded, and corrected for dead pixels by interpolating over neighboring pixels. The subsequent steps follow the method developed by Labeyrie (1970) to compute the square of the Fourier amplitudes $|\tilde{O}(f)|^2$ for each star. Binary stars are differentiated from single stars by their distinct pattern in the power spectrum $|\tilde{O}(f)|^2$;

single stars exhibit a uniform $|\tilde{O}(f)|^2$, while a binary system displays a periodic $|\tilde{O}(f)|^2$ given by

$$|\tilde{O}(f)|^2 = \frac{R^2 + 1 + 2R\cos[2\pi\vec{\theta} \cdot \vec{f}]}{R^2 + 1 + 2R}, \quad (1)$$

where R is the flux ratio and $\vec{\theta}$ is the 2-dimensional separation on the sky. For stars with the characteristic sinusoidal fringe pattern of a binary, a chi-squared minimization of a two-dimensional model fit to the Fourier amplitudes provides estimates of the flux ratio, separation, and position angle ($\pm 180^\circ$) of the binary (Ghez et al. 1995). The remaining 180° ambiguity in the position angle is eliminated by determining the Fourier phases as prescribed by Lohmann et al. (1983). Examples of two speckle binaries with different separations and position angles are shown in Figure 1.

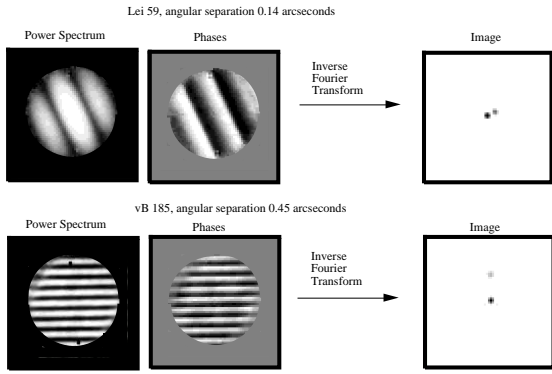


Figure 1: Two example speckle imaging reconstructions are shown for the Hyades binaries vB 24 and vB 185. The left fringe pattern displays the calibrated Fourier amplitudes $|\tilde{O}(f)|^2$, and the right fringe pattern displays the Fourier phases ($\arg\tilde{O}(f)$). Using an inverse Fourier transform, the diffraction-limited image of each binary is produced.

The separation and flux ratio are well-determined by the model fit for systems in which the first minimum occurs at a spatial frequency less than D/λ , equivalent to a separation greater than $\lambda/2D$ (*i.e.* $> 0''.05$). Three stars – vB 91 vB 96, and +10 568 – which have formal separation solutions of exactly the theoretical resolution limit in the Palomar data, $0''.05$, may actually have slightly different separations, since the data does not show if the decline in the Fourier amplitudes extends entirely to the first minimum. These stars were reobserved with the 10m Keck telescope in 1996 and 1997, one to three years after the initial Palomar observations and the more accurate flux ratios determined from the Keck data are used to refine the Palomar measurement of the separations. The separation of vB 91 and vB 96 stars increased in the 1996 data, probably as a consequence of orbital motion. The Keck measurements are reported in Table 3, but the statistical analysis described in §6 is restricted to the Palomar results in order to maintain a consistent set of data.

For the widest binaries, the magnitude difference estimate from the model fit method is overestimated; this occurs because some of the flux in the speckle cloud of wide companions

falls outside the array and because the images are apodized before their power spectra are computed. To avoid this bias, the binaries with separations wider than one-half the field of view minus one-half the speckle cloud size (*i.e.* $> 0''.70$) are reanalyzed with the shift and add technique (cf. e.g. Bates & Cady 1980; Christou 1991). The systems analyzed with this technique are vB 40, vB 17, vB 151, Lei 52, Lei 130, +22 669, vB 52, and vB 5, as noted in Table 3. As expected, the shift and add ΔK values are all smaller than the results from the speckle analysis, although the differences between the two methods are only significant for separations larger than $1''.0$.

The final step in the data analysis computes the limits for possible unseen companions to the single stars. These limits vary with atmospheric conditions, the target star brightness, and the distance from the target star. The companion detection limits, ΔK_{lim} , of each single star observation is found by solving for the maximum amplitudes of several cosine waves corresponding to a separations of $0''.05$, $0''.06$, $0''.07$, $0''.10$, $0''.15$, and $0''.60$ that could be hidden in the noise of the Fourier amplitudes. The method is similar to that described in Ghez et al. (1993) and Henry (1991), but the maximum simulated cosine waves are only allowed to vary from 3 times the rms scatter to unity rather than from the lowest power spectrum value to unity.

5. Results

5.1. IR Speckle Results

Of the 167 stars observed, 33 are resolved as binary systems; nearly half of the binaries, 12 systems, are new detections. The properties of the speckle binaries are listed in Table 3 and each binary is plotted in Figure 2. The smallest separation measured was $0''.044$, and the largest K magnitude difference measured was 5.5 mag, which corresponds to a companion mass of only $0.10 M_{\odot}$ and a mass ratio of 0.13 (see Appendix). The faintest companion has an apparent K magnitude of 12.8. Each detected pair is assumed to be bound, since the probability of a chance superposition is only $\sim .01\%$ given the $\sim 4 \times 10^{-5}$ per square arcsecond surface density of field stars with $K < 12$ in the direction of the Hyades (Simon et al. 1992).

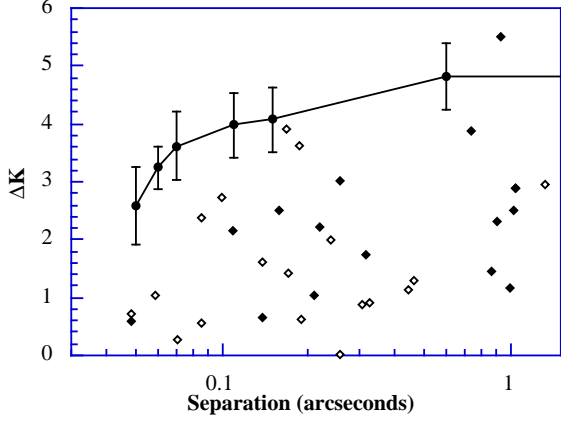


Figure 2: The observed properties for the 33 detected binaries (new binaries – filled diamonds, known binaries – open diamonds) are compared to the median companion star detection limits (filled circles) at several separations. The error bars are the standard deviations of the limits. At the completeness limit of the survey, $0''.10$, the observations are, on average, sufficiently sensitive to detect a binary star with a magnitude difference of $\Delta K = 4$.

Before discussing the statistical properties of the Hyades binaries in the speckle sample, an accurate accounting of the sensitivity of the observations is needed to define the separation and ΔK parameter space over which the survey is complete – the “completeness region.” The upper limit on the projected separation range is set by the camera field-of-view. With the target star image centered on the array, the upper cutoff is $1''.07$, one-half of the field-of-view with the finest pixel scale. The smallest angular separation reliably measurable with two-dimensional speckle imaging, with the assumption that the object Fourier amplitudes follow a binary star cosine pattern, is $\lambda/2D$, or $0''.05$. Although three binaries are resolved very close to this limit, many observations lack the sensitivity to detect companions at this extreme (see Table 4). The average sensitivity limit as a function of separation is shown in Figure 2, where the error bars represent the $1\text{-}\sigma$ rms variations in the sensitivity limits; these values are based on the ΔK_{lim} computed for the single stars. The completeness region lower cutoff is chosen to be $0''.10$ in order to maintain a nearly uniform sensitivity to companions at all separations. At this lower cutoff for the separation range the median ΔK_{lim} is 4.0 mag. At the distance of the Hyades, the angular separation range of the completeness region corresponds to a projected linear separation 5 to 50 AU. A total of 7 of the 33 pairs are detected outside the separation range of the completeness region and are therefore not included in the complete sample. Six of the binaries – vB 57, Lei 90, vB 91, +10 568, vB 120, and vB 96 – are omitted because their projected separations are less than the lower limit cutoff, while vB 40 is excluded from the complete sample because it has a separation larger than the upper limit cutoff.

In summary, over the binary star projected separation range of $0''.10$ to $1''.07$, the median of the detection limits is $\Delta K_{lim} = 4.0$ mag. At the distance of the Hyades, the angular separation range corresponds to a projected linear separation 5 to 50 AU. Based on the empirical mass- M_K relation described in the Appendix, the median magnitude

difference limit corresponds to a median mass ratio limit of 0.23. The derived detection limits and companion star masses are plotted in Figure 3 as a function of the target star mass. For the lowest mass stars in the sample, the median detection limit corresponds to companions of $\sim 0.2M_{\odot}$ – within $\sim 0.1 M_{\odot}$ of the hydrogen-burning limit. The higher mass stars, however, typically have detection limits that only extend to $\sim 0.6M_{\odot}$ – comparable to the primary mass of the fainter stars in the survey.

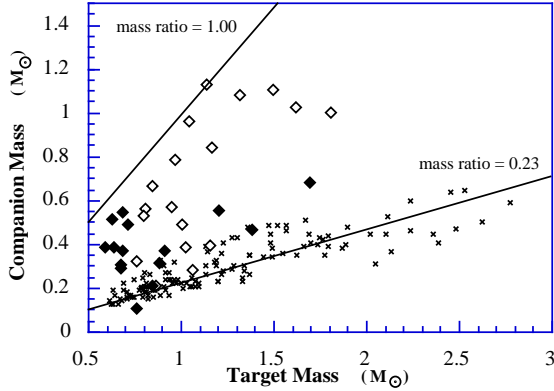


Figure 3: The derived primary and secondary masses for the speckle binary stars (new binaries - filled diamonds, known binaries - open diamonds) are plotted along with the companion star mass detection limits for the stars observed as single in the speckle survey (x). Although mass ratios as large as 0.13 are observed, the median mass ratio cutoff for this survey is 0.23.

5.2. Comparison with Previous Surveys

Previous investigations of the cluster multiplicity have utilized optical speckle, spectroscopy, and direct imaging, and in this section the results of several such studies are compared to this project (see Table 3 & 4 notes). The optical speckle survey by Mason et al. (1993) includes most of our targets, with 133 stars in common. Twenty-eight of these 133 stars have been spatially resolved as binaries: 11 by both surveys, 4 stars – BD +35 714, vB 71, vB 41, and vB 132 – by Mason et al., and 13 by the current infrared (IR) survey alone. The 60% higher binary detection rate at IR wavelengths results from the enhanced sensitivity to smaller mass ratio main sequence binaries at longer wavelengths (see Appendix). The optical speckle survey detection limit, $\Delta V_{lim} = 3$, corresponds to a mass ratio of only 0.54, a factor of ~ 2 less sensitive in mass ratio than the present IR speckle observations. Of the 4 stars missed by this IR study, 2 are easily explained. Both vB 71 and vB 41 are giant stars which, unlike main sequence stars, require a larger dynamic range to observe a companion in the IR than at optical wavelengths. Additionally, the separation for vB 71, $0''.048$, is slightly below the limit observable with the present IR survey. The discrepancy with the stars +35 714 and vB 132 may result from either significant orbital motion or a ΔK greater than the limit listed in Table 3. The latter alternative seems unlikely, since the ΔK_{lim} of 4.5 and 3.1 in the current data implies ΔV detections greater than 7.0 and 4.7, both of which are beyond the detection limit of the optical speckle

results. Orbital motion, however, could position the companion star closer to the primary than the current IR speckle resolution in the three years between the optical and infrared measurements.

Repeated spectroscopic observations of many Hyades stars have been made by several authors (e.g. Griffin et al. 1988; Stefanik & Latham 1992); in general, radial velocity measurements detect short-period binaries unresolvable with speckle imaging. Nonetheless, many of the longer period spectroscopic binaries can, in principle, be spatially resolved. A 3 yr orbit represents the shortest-period orbit resolvable with this speckle survey, assuming a total system mass of $\sim 1M_{\odot}$ and the extreme conditions of an eccentricity near unity and a face-on orbit observed to have an angular separation of $0''.1$ at apastron. The minimum detectable period increases to ~ 9 yr for a circular orbit. Because of the incomplete overlap in separation range covered by speckle and spectroscopy, stars observed as binaries by both techniques can be either triples for which each technique detects a different pair of stars in the multiple system, or doubles for which the same pair is detected. The notes in Table 3 indicate which speckle binaries have also been measured spectroscopically and which binaries are actually triple systems with separate speckle and spectroscopic pairs.

The common sample between the IR speckle survey and the Griffin et al. (1988) radial velocity survey contains 87 stars. Of the 33 Griffin et al. binaries in this set, 15 are also resolved by the speckle measurements. The separation and period are so discrepant for 8 of the 15 speckle/spectroscopic binaries – Lei 20, 22 669, vB 40, Lei 83, vB 124, vB 185, vB 102, and vB 151 – that they must be triple stars consisting of a spectroscopic binary and a third star orbiting further away. The remaining 7 binaries resolved by both surveys – vB 57, vB 113, Lei 90, vB 96, vB 114, vB 59, and vB 91 – are systems for which the two techniques are probably detecting the same pair. Five spectroscopic systems – vB 115, Lei 57, vB 106, vB 71, and vB 39 – have periods >3 yrs, but were not resolved by the IR speckle survey; vB 71 has already been discussed (see comparison with optical speckle), and the rest may be at orbital positions which correspond to a separations below the resolution limit of the IR speckle measurements or they may be single-lined binaries with faint companions.

An additional 11 spectroscopic binaries in the speckle sample are listed in Stefanik & Latham (1992) and 6 of these systems were resolved with the speckle observations. All 6 binaries resolved with speckle – vB 24, vB 29, vB 58, vB 75, vB 122, and vB 124 – have orbital periods consistent with the observed speckle separations, so it is unlikely that any are triple stars. Despite the long period of vB 131, it was not resolved. The four remaining systems have such short periods that they are unresolvable with these speckle observations, and one of the short-period binaries – vB 34 – also has a white dwarf companion (Bohm-Vitense 1993), making it a triple system. A second star in the speckle

sample has a white dwarf companion – +16 516 (V471 Tau Nelson & Young 1976). Another 8 spectroscopic systems are listed in Barrado y Navascues & Stauffer (1997). Although the orbital periods are not given, 4 of the spectroscopic binaries – vB 81, vB 50, vB 52, and vB 120 – were resolved with speckle, and are assumed to be double, not triple, stars. Five additional early-type spectroscopic systems with known periods are noted in Table 4, and the periods are given in Abt (1965), Abt & Levy (1985), and Burkhart & Coupry (1989). The 17 pairs detected by both speckle and spectroscopy provide a rare opportunity to accurately determine the mass and distance of each star without relying on additional assumptions about the stars or the Hyades cluster. Two such studies have already been carried out for vB 57 and vB 24 (Torres et al. 1997a,b).

Although more than one-half the current sample has been studied recently with spectroscopy, current direct imaging surveys of the Hyades have concentrated on the lower luminosity stars beyond the magnitude limit of the speckle survey. For example, the imaging survey by Macintosh et al. (1997) includes only 39 of the stars in the speckle sample. Four of the stars in common – vB 99, vB 105, vB 109, and vB 7 – had candidate companions, but their large angular separations make it unlikely that any of the pairs are physically associated. Another direct imaging survey of the Hyades involving HST observations does not include any of the stars in this survey (Gizis & Reid 1995; Reid & Gizis 1997). Early photographic surveys were capable of detecting bright ($B < 12$) companions at modest separations ($> 5'' - 10''$) among the brighter stars, but these stars are heavily saturated on deeper plates. Thirty-six of the stars in the speckle survey are listed in the ADS or IDS catalogues as visual doubles or triples with separations ranging from $0''.1$ to $88''.6$ (Aitken 1932; Jeffers, van den Bos & Greeby 1963). The eight systems in these catalogues with separations less than $1''.5$ – vB 29, vB 40, vB 57, vB 58, vB 75, vB 122, vB 124, and vB 132 – have been resolved with either optical or infrared speckle and are close enough to be considered physically associated (see §5.1). Most of the wider “companions,” however, are not Hyades members and are therefore discounted. Of the 7 visual binaries for which both stars are definite Hyades members – vB 1/vB 2, vB 71/vB 72, vB 83/vB 182, vB11/vB 12, vB 54/vB 55, vB 56/vA 354, and vB 131/vB 132 – only the $2''.0$ (~ 100 AU) vB 11/vB 12 system is considered a binary in the analysis of binary statistics. It is unlikely that the other 6 systems are physically associated because either the distance to each star is different by more than 3.5 pc (3σ) or the projected separation exceeds 4200 AU, the scale length between cluster members (Simon 1998).

Without considering the incompleteness of the different surveys, the total number of binary or multiple systems detected by spectroscopy, speckle, or direct imaging is 98 singles, 59 binaries, and 10 triples among the 167 stars including the evolved stars. After considering the results from other techniques, the 33 speckle binaries are actually 25 binaries

and 8 triples. Similarly, the 134 speckle singles become 98 singles and 34 binaries and 2 triples after including the other multiplicity data. Among the Hyades triple systems, all are hierarchical. The triple with the most similar separations is vB 102 with a 731 day period spectroscopic pair and a third star resolved by speckle at a distance of $0''.24$, implying a ratio of semi-major axes of $\sim 8 : 1$

5.3. Improved Color-Magnitude Diagram

Unresolved binary stars significantly broaden the width of the main sequence, limiting the effectiveness of the color-magnitude diagram in studies of age variations and rapid rotation. With the combined data sets from radial velocity, speckle, and direct imaging, the color-magnitude diagram of the Hyades cluster can be improved by purging binaries from the graph. Since the widest binary has a separation of only $2''.0$, all companions are close enough to affect the photometry of the primary star. In addition to the effects of unresolved companions, the $\sim 2\%$ uncertainty in the distance measurements also contributes to the spread within the color-magnitude relation. Figure 4a shows the 167 stars in this sample including the measurements of the known multiples, and Figure 4b plots a noticeably narrower main sequence with only those stars with no known companions. Two stars remain significantly above the main sequence in Figure 4b – vB 60 and +13 647 – and are most likely unresolved binaries, although they are not counted as binaries in the analysis that follows. Neither of these sources has a reported spectroscopic measurement.

Excluding the two giants and the two stars above the main sequence in Figure 4b, the polynomial fit to the single star main sequence is

$$M_V = -0.16 + 9.0(B - V) - 2.6(B - V)^2. \quad (2)$$

The standard deviation of the difference between the measured M_V and the M_V expected from equation 2 is 0.12 for Figure 4a, half the scatter of 0.25 measured for Figure 4b. Although the Hyades cluster is too old to place a meaningful limit on the age spread, a similar reduction in the width of the main sequence will be important to constraining an age spread in younger clusters.

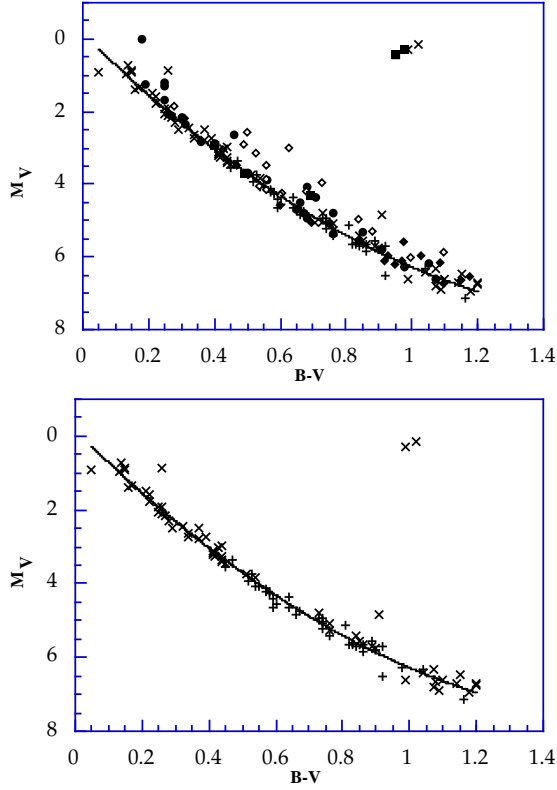


Figure 4a/b: Color-magnitude diagrams are shown for (a) all of the stars in the sample and (b) only those stars with no known companions. The symbols for binary stars are: filled circles – spectroscopic systems, filled squares – optical speckle system or visual binary, and diamonds – IR speckle binaries as in the previous figures.

Either the single stars have been observed with both speckle and spectroscopy (+), or they have been observed only with speckle (x). The width of the main sequence is reduced by a factor of 2 in Figure b, and the two stars located well above the main sequence in Figure b are probably photometric binaries.

6. Discussion

The following subsections examine the observed stellar properties in order to test the predictions of possible binary star formation and evolution scenarios. In §6.1 the companion star fraction (*csf*) of the sample is calculated and its dependence on radius (§6.1.1), mass (§6.1.2), and time (§6.1.3) are compared to theoretical models. The calculations in the discussion involving the *csf* consider all binaries detected with separations from $0''.10$ to $1''.07$. The mass ratio distribution and its radial and mass dependence are calculated in §6.2. The discussion describing the mass ratio distribution is also based on binaries in the $0''.10$ to $1''.07$ separation range, but the mass ratio range is restricted to 0.30 or larger. With the *csf* results, the mass ratio distributions are used to test several formation mechanisms.

6.1. Companion Star Fraction

The current sample covers a well-defined range of separation (5 to 50 AU) and mass ratio (~ 0.2 to 1.0), providing an excellent basis from which the multiplicity of the Hyades

can be determined. The number of companions can be quantified in two ways, the multiple star fraction or the companion star fraction. The multiple star fraction,

$$msf = \frac{b + t}{s + b + t}, \quad (3)$$

does not differentiate between different order multiple systems while the companion star fraction,

$$csf = \frac{b + 2t}{s + b + t}, \quad (4)$$

counts the total number of pairs, where s , b , and t are the number of singles, binaries, and triples. The uncertainties in the csf and msf are given by the Poisson counting error.

A lower limit on the Hyades main sequence multiplicity can be determined by combining the companions detected by the IR speckle survey with the additional companions discussed in §5.2. Outside the separation range of the speckle survey it is difficult to gauge the completeness, and no corrections are applied to account for undetected companions. Spectroscopic, speckle, and direct imaging surveys have revealed 96 singles, 57 binaries, and 9 triples among the current sample, excluding the giant stars. Given the total sample size of 162, the $msf_{total,obs}$ is 0.41 ± 0.05 , and the $csf_{total,obs}$ is 0.46 ± 0.05 . Because nearly one-half of the sample may not have been observed spectroscopically and all techniques have a limited sensitivity, the $msf_{total,obs}$ and $csf_{total,obs}$ are lower limits to the actual values.

Within the restricted separation range of $0''.10$ to $1''.07$ (5 to 50 AU), the observed $csf_{5-50AU,obs}$ and $msf_{5-50AU,obs}$ are 0.16 ± 0.03 (26 of 162 main sequence stars); the fractions are the same since no triple stars were resolved. Again, this value represents a lower limit on the total multiplicity between 5 and 50 AU, since faint companions are not detectable. The number of companions that lie within the separation range of this survey, but at magnitudes below our detection limit, is estimated by assuming that the companion K luminosity distribution follows an observed K luminosity distribution. The hypothesis that the magnitude distribution of companion stars resembles that of single stars is supported by the solar neighborhood G-dwarf survey which includes stars similar in mass to the Hyades survey (Duquennoy & Mayor 1991). The K-band luminosity function defined by all stars within 8 pc of the Sun is used to model the Hyades companion star distribution fainter than the detection limit (Reid & Gizis 1997, Henry & McCarthy 1992). The field luminosity function was selected instead of the Hyades K-band luminosity function because the observed population of Hyads is incomplete for the faintest stars, due to the greater difficulty in detecting these stars at further distances, and, possibly, due to the evaporation

of the lowest mass stars from the cluster (Reid 1993). Table 5 lists, for a given M_K , the percentage p of the field sample with fainter magnitudes, and the number N of speckle single stars in the Hyades sample with detection limits, M_{Klim} , from $(> M_K - 1)$ up to and including (M_K) . The percentage of the main sequence that is undetectable is determined by the average incompleteness,

$$incompleteness = \frac{\sum_{M_K=0.0}^{M_K=12.0} pN}{\sum_{M_K=0.0}^{M_K=12.0} N}. \quad (5)$$

For the 162 main sequence stars, the average percentage of the main sequence that is undetectable is 46%; dividing both the observed $csf_{5-50AU,obs}$ of 0.16 ± 0.03 and the uncertainty by 0.54 to account for missing stellar companions yields a $csf_{5-50AU,corr}$ of 0.30 ± 0.06 over the projected separation range of 5 to 50 AU. Since the total Hyades sample is divided into several subsamples in the following sections, the detection limit groupings for each subsample are also listed in Table 5 as is the final assessment of the subsample incompleteness. In the following discussion, these subsamples are used to study binary star formation mechanisms and possible evolutionary effects.

6.1.1. Radial Distribution of Multiple Systems – Imprint of Star Formation or Ongoing Relaxation?

Evidence of mass segregation, a concentration of the higher mass stars at the cluster center, has already been observed in the Hyades (Reid 1992), and a similar segregation of the binaries is expected if the former result is due to cluster relaxation. Alternatively, high mass stars may preferentially form at the cluster center as a consequence of enhanced accretion occurring in the region of highest gravitational potential (Bonnell et al. 1997; Zinnecker 1982). If the second scenario is responsible for the mass segregation, then the binaries are not expected to be concentrated toward the central region of the cluster.

To investigate the radial distribution of multiple stars in the Hyades, the multiplicity inside and outside of 3 pc are compared. The dividing radius is chosen to be 3 pc since the mass function for the main sequence sample inside this radius is significantly different from the mass function outside this radius – evidence of mass segregation. The coordinates given in Gunn et al. (1988) are taken as the center of the Hyades cluster and a distance of 46.3 pc to the center is assumed. The results, listed in Table 6, show no difference between the central and outer binary fraction of either the complete speckle sample or the total binary/multiple sample which incorporates several techniques; varying the dividing radius

does not alter the result. Although this result is consistent with the competitive accretion model, the statistical significance of the conclusion is low given that the secondary stars add an average of only 40 % to the total mass of the system. A larger sample size would improve the significance of this conclusion. The lack of a radial dependence in the csf is, however, consistent with the observed mass segregation in clusters that are sufficiently young that dynamical evolution cannot have caused the higher mass stars to migrate toward the center (e.g. Hillenbrand 1997, Sagar et al. 1988).

6.1.2. *Mass Dependence of the Companion Star Fraction – an Observational Test of Scale-Free Fragmentation and Small-N Capture*

Certain binary star formation models predict distinct mass dependences for the companion star fraction; scale-free fragmentation models produce binaries with properties that are independent of the primary mass (Clarke 1998), while capture in small clusters preferentially forms binaries among the highest mass stars (McDonald & Clarke 1995). Based on theoretical calculations by Clarke designed for comparison to data sets with a constant mass ratio cutoff, the speckle sample csf_{obs} should be independent of primary mass in the case of scale-free fragmentation, whereas the same csf_{obs} should increase with increasing primary mass for capture in small-N (4-10 star) clusters. To test the predictions of the two models, the sample is split in two by B-V color in increments of 0.10 and the csf for the stars bluer and redder than the cutoff is determined. For all B-V cutoffs, the bluer (higher mass) stars have a consistently smaller csf than the redder (lower mass) stars, although the difference is never statistically significant. Table 6 lists the csf_{obs} and csf_{corr} for three B-V ranges (used in §6.1.3) for both the complete speckle binary sample and the total binary/multiple sample. The csf of the more massive stars is not larger than that of the less massive stars, contradicting the expectation of the small-N capture model. Although the paucity of substellar companions detected in large surveys (e.g. Nakajima et al. 1995, Macintosh et al. 1997, Zuckerman & Becklin 1992) suggests that binary formation is not entirely scale-free, the results from this survey support the scale-free fragmentation model of formation for stars in the mass range of the survey, $\sim 0.6M_{\odot}$ to $2.8M_{\odot}$.

6.1.3. *Evolution of the Companion Star Fraction*

The companion star fraction has been observed to differ significantly between the pre-main sequence and main sequence stage of stellar evolution, with a larger proportion of binaries among the younger population. One proposed explanation for this discrepancy

is the disruption of primordial multiple star systems over time which could be reflected in an intermediate *csf* for the Hyades sample (Ghez et al. 1993). Among the alternate explanations are: an environmental effect involving the different types of star forming regions and a result of the shape of the evolutionary tracks which map a wider range of companion masses into a given detection limit at the pre-main sequence stage (Ghez 1996). Ideally, any comparison between samples of different ages is made over a common range of separation and sensitivity. For this study, 5 to 50 AU defines the separation range, and mass ratios from ~ 0.2 to 1.0 set the limits of the sensitivity range.

A comparison set of the pre-main sequence binaries is taken from both lunar occultation and speckle surveys of T Tauri stars in the Taurus and Ophiuchus star-forming regions (Ghez et al. 1993; Leinert et al. 1993; Simon et al. 1995). Since the nearest star-forming regions are three times as distant as the Hyades, the combination of lunar occultation and speckle ensures that the entire 5 to 50 AU separation range is covered. Because K magnitudes do not uniquely determine the mass of a T Tauri star, the *csf* of the T Tauri stars is calculated by grouping the observations by their detection limits and then dividing the number of binaries with a certain range of flux ratios by the number of observations with the sensitivity to detect a companion in that flux ratio range (cf. Ghez et al. 1997). The resulting companion star fraction for the ~ 2 Myr-old pre-main sequence sample is $csf_{5-50AU,TTauri} = 0.40 \pm 0.08$.

The older, ~ 5 Gyr-old comparison sample is taken from the multiplicity survey of the solar neighborhood G-dwarfs (Duquennoy & Mayor 1991). These data cover 10 orders of magnitude in orbital period, but the range 3.7 to 5.2 $\log P$ [dys] corresponds to a projected linear separation range of 5 to 50 AU, assuming a system mass of $1.4 M_{\odot}$ (the average value for the G-dwarf sample) and a factor of 1.26 between the projected separation and the semi-major axis (Fischer & Marcy 1992). Although this period range encompasses the results of two observing techniques, spectroscopy and direct imaging, used in the G-dwarf survey, the majority of this range is covered by direct imaging. The G-dwarf visual binary companion correction limit of $\Delta V = 7$ mag is comparable to the median Hyades limit of $\Delta K = 4$ mag (see Appendix). The *csf* for the older solar neighborhood (SN) sample was calculated by integrating the Gaussian fit to the corrected numbers of pairs in the G-dwarf survey over the period range 3.7 to 5.2 $\log P$ [dys], yielding a $csf_{5-50AU,SN}$ of 0.14 ± 0.03 . Preliminary results from a survey of solar neighborhood K stars yields a very similar binary distribution (Mayor et al. 1992), so the $csf_{5-50AU,SN}$ should represent the *csf* for nearby stars with spectral types from F7 to K.

Recently, 144 Pleiades G and K dwarfs were observed with adaptive optics at the CFHT by Bouvier et al. (1997). These observations cover neither the same separation range

nor the same range of sensitivity, complicating any comparison between this data set and the Hyades speckle results. Due to the greater distance to the Pleiades, the minimum binary star separation observed in the Pleiades is 11 AU. In the Hyades survey presented here, 42% of the speckle binaries have separations within the missing 5 to 11 AU range. Unlike the G-dwarf survey which has a comparable sensitivity to the Hyades IR speckle survey, the Pleiades observations have a detection limit of at most $\Delta K = 2$ mag in the 11 to 50 AU range. The CFHT results have been corrected to allow for lower-mass companions (to the Hydrogen-burning limit) under the assumption that the companion star mass function is the same as that of field stars (the procedure used to determine the Hyades $csf_{total,obs}$ in §6.2 gives the same correction for the Pleiades as the one listed in the Bouvier et al. paper). This procedure results in very substantial corrections. Within the separation range overlapping the Hyades sample (11-50 AU), 7 binaries were observed, but an additional 12 undetected binaries are predicted. Including corrections for both the missing separations and the undetectable companions, the $csf_{5-50AU,Pleiades}$ is 0.23 ± 0.09 . More sensitive observations are required before it is possible to make a statistically significant comparison with the current Hyades data.

Incorporating the results of the T Tauri, Hyades, and Solar Neighborhood surveys, Figure 5 shows the fraction of binaries with separations from 5 to 50 AU as a function of age. Because the comparison samples cover different mass and sensitivity ranges, two values are computed for the Hyades sample. Since the T Tauri stars evolve into stars with masses $< 3M_{\odot}$ and it is easier to detect low mass companions when they are young (Ghez, White & Simon 1997), the most appropriate Hyades csf is the entire main sequence sample (primary mass $\sim 0.6M_{\odot}$ to $2.8M_{\odot}$) corrected to account for missing main sequence companions, $csf_{5-50AU,corr}$ of 0.30 ± 0.06 . The solar neighborhood comparison is more direct since the Duquennoy & Mayor (1991) sample has the same sensitivity level as the speckle observations and includes stars from F7 to G9 (with similar results for K stars – Mayor et al. 1992). The Hyades $csf_{5-50AU,obs}$ determined from the subset of 107 Hyades stars with (B-V) colors consistent with spectral types from F7 to K5 is most analogous to the solar neighborhood csf and equals 0.21 ± 0.04 . Although the statistical significance of the differences are not high ($< 2\sigma$), the Hyades csf is between the younger and older samples and may suggest a downward trend in multiplicity. Observations of clusters with ages between the Hyades and T Tauri stars which cover a similar separation and sensitivity range are required to clearly establish whether or not an evolutionary trend in the companion star fraction exists.

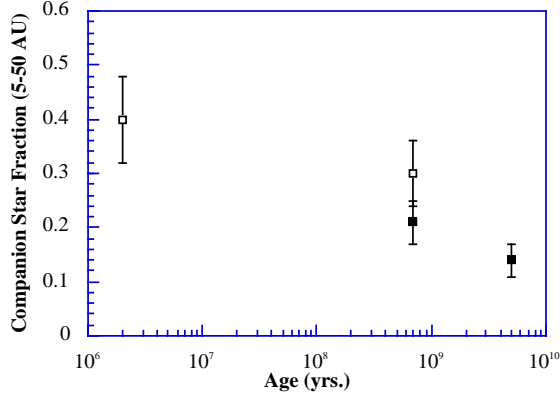


Figure 5: The csf_{5-50AU} for three stellar samples is plotted as a function of the sample age. Open squares signify the csf of stars with masses from $\sim 0.5M_{\odot}$ to $\sim 3M_{\odot}$, the full range of the sample, which overlaps the mass range of T Tauri stars. The Hyades value has been corrected to account for all stellar companions, and the corrected T Tauri value has a similar sensitivity. Filled squares represent the

csf_{5-50AU} of late-F through K stars, the spectral type range covered by the Duquennoy & Mayor (1991) solar neighborhood survey. The Hyades value is not corrected since the Hyades survey has a detection limit comparable to that reported for the solar neighborhood results. The figure is suggestive of an evolutionary trend in multiplicity, although the csf_{5-50AU} measured for the Hyades is not significantly different from the csf_{5-50AU} of the older solar neighborhood.

6.2. Mass Ratio Distribution – an Observational Test of Several Binary Star Formation Mechanisms

The mass ratio (q) distribution and its dependence on separation, primary mass, and radial distance provide additional constraints on several binary star formation theories. The mass ratio distribution for all binaries with separations from 5 to 50 AU is shown in Figure 6 and increases toward smaller mass ratios from 1.00 down to a ratio of 0.30. The decrease in the distribution for mass ratios below 0.3 is due to incompleteness. Only half of the observations are sensitive to mass ratios of 0.23, whereas *all* the observations are sensitive to mass ratios greater than 0.30. To avoid any observational bias, this analysis is restricted to mass ratios from 0.30 to 1.00. The best fit power law description of the data is $q^{-1.3 \pm 0.3}$ which has a K-S test probability of 89%.

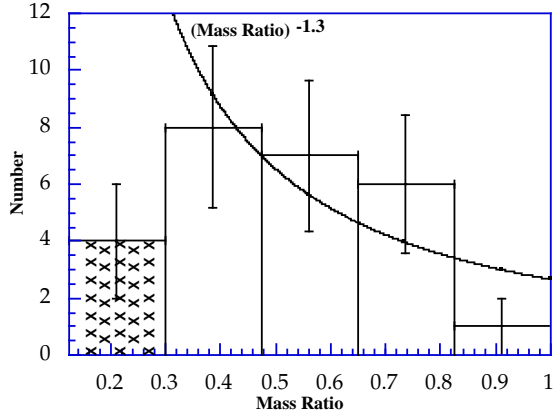


Figure 6: A histogram of mass ratios, q , for the binaries with separations from $0''.10$ to $1''.07$ is shown. Since all the observations in the survey are sensitive enough to detect a binary with a mass ratio of 0.30, only the 22 binaries with mass ratios larger than 0.30 were involved in determining the fit to the mass ratio distribution. The additional 4 systems with smaller mass ratios are included in

the graph, but the bin containing these binaries is marked with x's since the survey is not complete at this mass ratio extreme. The best fit power law of $q^{-1.3}$ is also shown.

This declining power law is inconsistent with the flat or slightly rising distributions of both 30 Pleiades F7-K0 spectroscopic and photometric binaries and 23 solar neighborhood G-dwarf spectroscopic systems (Mermilliod et al. 1992, Mazeh et al. 1992). The distribution of the 23 G-dwarf binaries with periods less than 3000 days was found to be different from the long period distribution of G-dwarf binaries. Dividing the complete sample of Hyades speckle binaries in half based on separation showed no evidence of a separation dependence for the mass ratio distribution; the K-S probability that the two separation distribution are the same is 89%. Because the separation range of the speckle observations is limited to 45 AU, comparison with spectroscopic or visual binaries may be required to test for a difference in the mass ratio distributions. This comparison, however, has the advantage of studying distributions of mass ratios constructed with binaries detected by the same technique.

The mass ratio distribution also shows no dependence on either primary star mass or radial distance. To investigate the mass dependence of the distribution, the binaries are divided in half based on their primary mass and a K-S test indicates that the mass ratio distributions for high and low mass primaries have an 81% probability of being the same; there is no mass dependence of the mass ratio distribution. Similarly, the mass ratio distribution does not depend on radial distance; the half of the binaries with smaller radial distances has an 81% probability of being drawn from the same distribution as the half of the binaries with larger radial distances.

Both the scale-free fragmentation model and capture in small-N clusters make specific predictions that can be compared to the observational results described above. For binaries formed by scale-free fragmentation, the mass ratio distribution is expected to be independent of, or only weakly dependent on, the primary star mass (Clarke 1998), consistent with the Hyades data. This formation scenario is also consistent with the

observation that the csf is independent of mass. Diskless capture in small-N clusters tends to form binaries consisting of the two most massive stars (McDonald & Clarke 1995), causing the distribution to increase towards large mass ratios; with its negative slope, the Hyades mass ratio distribution, like the csf in §6.1.2, does not support this model.

Simulations of accretion during binary formation also predict measurable effects in the mass ratio distribution. This model suggests that accretion of high angular momentum circumbinary material drives the mass ratio toward unity, while accretion of low angular momentum circumstellar material results in smaller mass ratios (Bate & Bonnell 1997). The Hyades data suggest that few binaries have accreted a large amount of circumbinary material. A number of scenarios such as scale dependent fragmentation and disk fragmentation (cf. Boss & Myhill 1995, Myhill & Kaula 1992, Burkert & Bodenheimer 1996, Bonnell & Bate 1994) which lack observational predictions remain possible formation mechanisms in addition to the scale-free fragmentation model.

7. Summary

Infrared speckle observations of 167 bright Hyades members, approximately one-third of the cluster, were made with the Hale 5m telescope. A total of 33 binaries were resolved, of which 13 are new detections, and an additional 17 are known spectroscopic binaries. Including the results from spectroscopic and direct imaging surveys, the ratio of singles:binaries:triples in the sample is 98:59:10.

Over the separation range $0''.10$ to $1''.07$, the observations are sensitive to companions 4 mag fainter than the target star. Within this separation range, 26 of the 162 main sequence stars are resolved as binaries, resulting in an observed $csf_{5-50AU,corr}$ of 0.16 ± 0.03 ; accounting for the inability to detect fainter companions increases the multiplicity to $csf_{5-50AU,total}$ of 0.30 ± 0.06 . The Hyades csf is intermediate between the fractions of the younger T Tauri stars and the older solar neighborhood. Although the observations permit an evolutionary trend in multiplicity, this result is not conclusive and future observations of other young clusters will further illuminate this discussion.

Within the Hyades speckle sample, the csf is independent of radial distance and primary star mass. Another key observational result is the mass ratio distribution. Unlike spectroscopic studies which are biased because of the uncertainty of the inclination angle, the resolved speckle binaries provide mass ratios that are free of selection effects from ratios of 0.30 to 1.00. The observed mass ratio distribution is best described by a power law $q^{-1.3 \pm 0.3}$. This mass ratio distribution does not vary with primary star mass, binary

star separation or distance from the cluster center. Comparing models of accretion during binary formation to the observed mass ratio distribution leads to the conclusion that few binaries experience accretion of high angular momentum material. Overall, the Hyades data support the scale-free fragmentation model, but not capture in small-N clusters or disk-assisted capture in small-N clusters (McDonald & Clarke 1993, 1995; Clarke 1998). In addition to scale-free fragmentation, binary star formation mechanisms not rejected by the Hyades data are scale dependent fragmentation and disk fragmentation, scenarios for which there are currently no observational tests (cf. Boss & Myhill 1995, Myhill & Kaula 1992, Burkert & Bodenheimer 1996, Bonnell & Bate 1994).

Support for this work was provided by NASA through grant number NAGW-4770 under the Origins of Solar Systems Program. We thank the staff at Palomar for their assistance with our observations. This research required extensive use of the SIMBAD database, operated at CDS, Strasbourg, France.

A. An Empirical Mass- M_K Relation

The results and limitations of this survey are transformed into physical parameters through an empirical mass- M_K relation. Since this relation varies with age and metallicity, the ideal relation would be constructed from Hyades stars. Although the nearby star samples do not have the same age and metallicity as the Hyades, the masses of a number of these stars have been determined (Andersen 1991, Henry & McCarthy 1993), and the empirical relation used for the Hyades stars is based on solar neighborhood surveys. Because many of the stars in the Hyades sample have $M_K < 3.07$, the relations derived by Henry & McCarthy (1993) cannot be applied to the entire sample. An alternate mass- M_K relation was constructed by combining the low mass Henry & McCarthy data with the higher mass data listed for Main Sequence detached eclipsing binaries in the review by Andersen. The M_V given for each star in the more massive systems was converted into an M_K based on a color-color relation constructed with the data compiled in Kenyon & Hartmann (1995). The linear fit to the B-V and V-K data listed for A through K stars is

$$(V - K) = 2.38(B - V) + 0.03. \quad (\text{A1})$$

A single line was used to fit the A through M star data rather than a combination of three lines as in Henry & McCarthy (1992), and the resulting mass- M_K relation is

$$\log(M/M_{\odot}) = -0.159M_K + 0.49. \quad (\text{A2})$$

This relation is used to convert each observed binary ΔK or single ΔK_{lim} into a mass ratio or a mass ratio detection limit. For fainter magnitudes, the fit predicts that the Hydrogen-burning limit of $0.08M_{\odot}$ occurs at $M_K \sim 10$. For brighter magnitudes, the recently-determined dynamical masses for the components of vB 24 and vB 57 provide a check on the empirical relation at higher masses (Torres et al. 1997a,b). For both binaries, the photometric masses derived from the infrared speckle measurements match the dynamical values almost exactly for the primary mass. The average discrepancy in the secondary mass is 23%, and this value is taken as the uncertainty in the measurements of the secondary masses and the mass ratios.

An empirical mass - M_V relation, also constructed from the same data set, is necessary to compare the infrared observations presented here with the previous work done at optical wavelengths. The mass- M_V relation is

$$\log(M/M_{\odot}) = -0.090M_V + 0.45. \quad (\text{A3})$$

Because the mass- M_V relation has a shallower slope than the corresponding mass- M_K relation, a larger ΔV than a ΔK detection limit is required to reach the same companion mass. Due to this effect, an optical speckle survey with similar dynamic range as the infrared speckle observations, is much less sensitive to low mass companions. With a detection limit of $\Delta V = 3$, the optical speckle survey conducted by Mason et al. (1993) has a mass ratio limit of 0.54. The visual pair binaries in the Duquennoy & Mayor (1991) survey were corrected to a larger value of ΔV , 7 mag, which corresponds to a mass ratio limit of 0.23, similar to the Hyades survey. Both the G-dwarf and the Hyades surveys are sensitive to companions as faint as early M stars.

REFERENCES

- Abt, H. A. & Levy, S. G. 1985, ApJS, 59, 229.
- Abt, H. A. & Levy, S. G. 1976, ApJS, 30, 273.
- Abt, H. A. 1965, ApJS, 102, 429.
- Aitken, R. G. 1932, *New General Catalogue of Double Stars*, Carnegie Institution of Washington.
- Andersen, J. 1991, A&A Rev., 3, 91.
- Barrado y Navascues, D. & Stauffer, J. R. 1997, A&A, 310, 879.
- Bate, M. R. & Bonnell, I. A. 1997, MNRAS, 285, 33.
- Bate, M. R., Bonnell, I. A., & Price, N. M. 1995, MNRAS, 277, 362.
- Bates, R. H. T. & Cady, F. M. 1980, Opt. Comm., 32, 365.
- Bohm-Vitense, 1993, AJ, 106, 113.
- Bonnell, I. A. & Bate, M. R. 1994, MNRAS, 269, L45.
- Bonnell, I. A., Bate, M. R., Clarke, C. J. & Pringle, J. E. 1997, MNRAS, 285, 201
- Boss, A. P. & Myhill, E. A. 1995, ApJ, 451, 218.
- Bouvier, J., Rigaut, F. & Nadeau, D. 1997, A&A, 323, 139.
- Burkert, A. & Bodenheimer, P. 1996, MNRAS, 280, 1190.
- Burkhart, C. & Coupry, M. F. 1989, A&A, 220, 197.
- Christou, J. C. 1991, PASP, 103, 1040.
- Clarke, C. 1996, in *Evolutionary Processes in Binary Stars*, eds. Wijers, R. A. M. J., Davies, M. B., and Tout, C. A.
- Clarke, C. J. 1998, MNRAS, in press.
- Duquennoy, A. & Mayor, M. 1991, A&A, 248, 485.
- Fischer, D. A. & Marcy, G. W. 1992, ApJ, 396, 178.
- Ghez, A.M., Neugebauer, G., & Matthews, K. 1993, AJ, 106, 2005.
- Ghez, A. M. 1996, in *Evolutionary Processes in Binary Stars*, eds. Wijers, R. A. M. J., Davies, M. B., and Tout, C. A.
- Ghez, A. M., McCarthy, D. W., Patience, J. L. & Beck, T. L. 1997, ApJ, 481, 378
- Ghez, A. M., Weinberger, A. J., Neugebauer, G., Matthews, K., & McCarthy, D. W. 1995, AJ, 110, 753.

- Ghez, A. M., White, R. J., & Simon, M. ApJ, 1997, 490, 353.
- Gizis, J. & Reid, I. N. 1995 AJ, 110, 1248.
- Griffin, R. F., Gunn, J. E., Zimmerman, B. A. & Griffin, R. E. M. 1988, AJ, 96, 172.
- Griffin, R. F., Gunn, J. E., Zimmerman, B. A. & Griffin, R. E. M. 1985, AJ, 90, 609.
- Griffin, R. F., Mayor, M. & Gunn, J. E. 1982, A&A, 106, 221.
- Griffin, R. F. & Gunn, J. E. 1981, AJ, 86, 588.
- Griffin, R. F. & Gunn, J. E. 1978, AJ, 83, 1114.
- Gunn, J. E, Griffin, R. F., Griffin, R. E. M., & Zimmerman, B. A. 1988, AJ, 96, 198.
- Henry, T. J. & McCarthy, D. W. 1993, AJ, 106, 773.
- Henry, T. J. & McCarthy, D. W. 1992, in *Complimentary Approaches to Double and Multiple Star Research IAU Colloquium 135*, eds. McAlister, H. A. & Hartkopf, W. I.
- Henry, T. J. 1991, Ph. D. thesis, University of Arizona.
- Hillenbrand, L. A. 1997, AJ, 113, 1733.
- Jeffers, H. M., van den Bos, W. H. & Greeby, F. M. 1963, *Index Catalogue of Visual Double Stars 1961.0*, University of California Publication of the Lick Observatory.
- Kenyon, S. J. & Hartmann, L. 1995, ApJS, 101, 117.
- Labeyrie, A. 1970, A&A, 6, 85.
- Leinert, Ch., Zinnecker, H., Weitzel, N., Christou, J., Ridgway, S. T., Jameson, R., Haas, M., & Lenzen, R. 1993, A&A, 278, 129
- Lohmann, A. W., Weigelt, G. & Wirtzner, B. 1983, App. Opt., 22, 4028.
- Macintosh, B., Zuckerman, B., Becklin, E., McLean, I., 1997, ApJsubmitted.
- Mason, B. D., McAlister, H. A., Hartkoff, W. I., & Bagnuolo, W. G. Jr. 1993, AJ, 105, 220.
- Matheiu, R. D. 1994, ARA&A, 32, 465.
- Matthews, K., Ghez, A. M., Weinberger, A. J., & Neugebauer, G. 1996, PASP, 108, 615.
- Mayor, M., Duquennoy, A., Halbwachs, J.-L., & Mermilliod, J.-C. 1992, in *Complimentary Approaches to Double and Multiple Star Research IAU Colloquium 135*, eds. McAlister, H. A. & Hartkopf, W. I.
- Mazeh, T., Goldberg, D., Duquennoy, A., & Mayor, M. 1992, ApJ, 401, 265.
- McDonald, J. M. & Clarke, C. J. 1993, MNRAS, 262, 800.
- McDonald, J. M. & Clarke, C. J. 1995, MNRAS, 275, 671.

- Mermilliod, J. C., Rosvick, J. M., Duquennoy, A., & Mayor, M. 1992, *A&A*, 265, 513.
- Mermilliod, J. C. 1976, *A&AS*, 24, 159.
- Myhill, E. A. & Kaula, W. M. 1992, *ApJ*, 386, 578.
- Nakajima, T., Oppenheimer, B. R., Kulkarni, S. R., Golimonski, D. A., Matthews, K., & Durrance, S. T. 1995, *Nature*, 378, 463.
- Nelson, B. & Young, A. 1976, in *Structure and Evolution of Close Binary Systems*, IAU Symposium No. 73, eds. Eggleton, P., Mitton, S., & Whelan, J.
- Pels, G., Oort, J. H., Pels-Kluyver, H. A. 1975, *A&A*, 43, 423.
- Perryman, M. A. C., Brown, A. G. A., Lebreton, Y., Gomez, A., Turon, C., Cayrel de Strobel, G., Mermilliod, J. C., Robichon, N., Kovalevsky, J., & Crifo, F. 1997, *A&A*, in press.
- Reid, I. N. 1992, *MNRAS*, 257, 257.
- Reid, I. N. 1993, *MNRAS*, 265, 785.
- Reid, I. N. & Gizis, J. E. 1997, *AJ*, 114, 1992.
- Sagar, R., Myakutin, V. I., Piskunov, A. E., and Dluzhnevskaya, O. B. 1988, *MNRAS*, 234, 831.
- Sanford, R. F. 1921, *ApJ*, 53, 201.
- Schwan, H. 1991, *A&A*, 243, 386.
- Simon, M., Chen, W. P., Howell, R. R., Benson, J. A., & Slowik, D. 1992, *ApJ*, 384, 212.
- Simon, M., Ghez, A. M., Leinert, Ch., Cassar, L., Chen, W. P., Howell, R. R., Jameson, R. F., Matthews, K., Neugebauer, G., & Richichi, A. 1995, *ApJ*, 443, 625.
- Simon, M. 1998, *ApJ*, in press.
- Stefanik, R. P. and Latham, D. W. 1992, in *Complementary Approaches to Double and Multiple Star Research IAU Colloquium 135*, eds. McAlister, H. A. and Hartkopf, W. I.
- Torres, G., Stefanik, R. P., & Latham, D. W. 1997a, *ApJ*, 479, 268.
- Torres, G., Stefanik, R. P., & Latham, D. W. 1997b, *ApJ*, 474, 256.
- van Bueren, H. G. 1952, *B. A. N.*, 432, 385.
- Zinnecker, H. 1982, in *Symposium on the Orion Nebula to Honor Henry Draper*, eds. Glassgold, A. E., Huggins, P. J., & Schucking, E. L.

Zuckerman, B. & Becklin, E. E. 1992, ApJ, 386, 260.

TABLE 1. Hyades Sample

Object	BD	HD	$\alpha(1950)^a$	$\delta(1950)^a$	V^b	B-V ^b	Sp. Ty. ^a	D(pc) ^c	K ^d
+20 480	+20 480	18404	2 55 14.0	20 28 08	5.79	0.41	F5	32.7	4.78
vB 1	+07 493	20430	3 14 46.0	07 28 24	7.39	0.57	F8	41.6	6.00
Lei 2			3 25 54.0	13 00 00	9.73	0.92	G0	42.6	7.51
+35 714	+35 714	21847	3 29 28.1	35 29 26	7.30	0.49	F8	50.7	6.10
vB 4	+23 465		3 29 52.9	23 31 27	8.89	0.84	G5	42.0	6.86
vB 5	+20 598		3 34 40.0	21 10 46	9.37	0.92	G5	43.1	7.15
+16 516	+16 516		3 47 36.0	17 04 00	9.51	0.85	K0	60.1	7.46
vB 170	+23 571		3 48 04.3	23 45 13	10.25	1.16	K7	40.8	7.46
vB 6	+16 523	24357	3 50 18.5	17 10 46	5.97	0.34	F4	42.8	5.13
vB 7	+16 529	285252	3 52 15.2	16 51 09	8.99	0.90	K2	42.0	6.82
vB 8	+09 524	25102	3 56 56.3	10 11 22	6.37	0.42	F5	42.1	5.34
Lei 11	+19 650		4 00 44.7	19 19 05	10.17	1.07	K5	45.2	7.60
Lei 10			4 02 46.9	17 48 11	9.30	0.89		50.2	7.15
vB 10	+15 582	25825	4 03 25.9	15 33 50	7.85	0.59	G0	46.8	6.42
Lei 15			4 04 11.3	15 12 07	10.49	1.18		49.1	7.65
Lei 16	+16 558		4 04 52.0	16 23 11	9.94	0.99	K0	45.2	7.56
vB 11	+14 657A	26015	4 04 52.2	15 01 51	6.02	0.40	F0	40.4	5.04
+13 647	+13 647		4 05 30.6	13 23 31	8.81	0.91	G5	59.6	6.62
Lei 18			4 05 36.5	23 38 13	9.44	0.90		53.1	7.27
+8 642	+8 642		4 07 05.9	09 10 30	10.10	1.20	K5	44.8	7.22
vB 13	+18 594	26345	4 07 49.0	18 17 38	6.62	0.42	F6	45.6	5.59
vB 14	+05 601	26462	4 08 40.7	05 23 39	5.72	0.36	F4	36.9	4.83
Lei 20			4 08 56.4	23 30 30	9.38	1.09	K2	42.6	6.76
vB 16	+22 657	26737	4 11 32.1	22 19 36	7.05	0.42	F5	58.0	6.02
vB 15	+23 649	26736	4 11 32.5	23 26 60	8.08	0.66	G5	43.3	6.48
vB 17	+14 673	26756	4 11 36.3	14 29 59	8.46	0.70	G5	45.7	6.77
vB 18	+12 566	26767	4 11 40.3	12 18 35	8.06	0.64	G0	46.9	6.51
vB 19	+10 551	26784	4 11 49.3	10 34 34	7.12	0.51	F8	45.4	5.88
vB 162	+20 721	26874	4 12 45.9	20 41 46	7.84	0.71	G4	47.4	6.12
vB 20	+15 603	26911	4 12 56.1	15 16 36	6.32	0.40	F5	47.0	5.34
vB 21	+21 612	284235	4 13 35.7	21 47 03	9.15	0.82	G5	48.6	7.17
vB 22	+16 577	27130	4 14 46.8	16 49 34	8.32	0.76	G8	49.1	6.48
vB 23	+17 703	27149	4 15 08.3	18 08 08	7.53	0.68	G5	47.6	5.88
+22 669	+22 669		4 15 11.1	23 09 48	9.48	0.98	K0	57.9	7.12
vB 24	+21 618	27176	4 15 25.7	21 27 30	5.65	0.28	F0	55.4	4.95
vB 25	+15 609	285690	4 15 28.1	15 58 02	9.59	0.98	K0	44.0	7.23
Lei 130			4 15 29.3	17 18 02	10.02	1.10		43.2	7.37
vB 26	+19 694	27250	4 16 02.3	19 47 10	8.63	0.74	G5	46.6	6.84
vB 27	+17 707	27282	4 16 15.2	17 24 16	8.43	0.73	G8	48.3	6.66
vB 28	+15 612	27371	4 16 57.0	15 30 29	3.65	0.99	K0 III	45.2	1.27
vB 29	+16 579	27383	4 17 03.2	16 24 10	6.89	0.56	F9	45.7	5.53
vB 30	+13 663	27397	4 17 08.9	13 54 57	5.59	0.28	F0	44.2	4.89
vB 31	+18 623	27406	4 17 18.1	19 06 52	7.47	0.57	G0	44.8	6.08
vB 32	+18 624	27429	4 17 30.9	18 37 26	6.13	0.37	F3	45.5	5.22
vB 33	+14 682	27499	4 17 46.3	14 58 38	5.26	0.22	F0	47.6	4.71
vB 34	+13 665	27483	4 18 04.2	13 44 49	6.17	0.46	F6	48.6	5.05
vB 35	+20 740	27524	4 18 34.6	20 55 21	6.80	0.44	F5	49.3	5.72
vB 36	+18 629	27534	4 18 38.3	18 17 59	6.81	0.44	F5	47.3	5.73
vB 37	+14 687	27561	4 18 45.6	14 17 32	6.61	0.41	F5	47.6	5.60
vB 38	+13 668	27628	4 19 14.7	13 57 36	5.72	0.31	A3 m	46.0	4.95
+10 568	+10 568	286770	4 19 39.7	11 11 21	9.81	1.18	K8	42.8	6.97
vB 39	+16 585	27685	4 19 52.6	16 40 29	7.86	0.68	G4	36.9	6.21

TABLE 1. (continued)

Object	BD	HD	$\alpha(1950)^a$	$\delta(1950)^a$	V^b	B-V ^b	Sp. Ty. ^a	D(pc) ^c	K^d
vB 40	+14 690	27691	4 19 54.0	14 56 24	6.99	0.56	G0	40.5	5.63
vB 41	+17 712	27697	4 20 03.2	17 25 35	3.76	0.98	K0 III	47.7	1.40
vB 42	+21 635	27732	4 20 24.7	21 15 48	8.85	0.76	G5	50.2	7.01
vB 43	+19 708	284414	4 20 27.4	19 32 34	9.40	0.91	K2	50.8	7.21
vB 44	+24 654	27731	4 20 29.1	24 17 23	7.18	0.45	F5	54.1	6.08
vB 45	+16 586	27749	4 20 33.0	16 39 41	5.64	0.30	A1 m	48.2	4.90
vB 46	+14 691	27771	4 20 42.6	14 33 18	9.11	0.86	G5	43.6	7.03
vB 47	+17 714	27819	4 21 12.9	17 19 45	4.80	0.16	A7	46.6	4.39
vB 48	+21 641	27808	4 21 16.4	21 37 17	7.13	0.52	F8	42.5	5.86
vB 49	+16 589	27835	4 21 21.1	16 15 52	8.24	0.59	G0	51.0	6.81
vB 50	+14 693	27836	4 21 22.6	14 38 38	7.62	0.60	G1	44.3	6.16
vB 174	+17 715		4 21 23.3	17 53 18	9.98	1.04	K5	52.1	7.48
vB 51	+16 591	27848	4 21 29.8	16 57 52	6.97	0.44	F8	50.0	5.89
vB 52	+16 592	27859	4 21 36.1	16 46 18	7.80	0.60	A2	42.4	6.34
vB 53	+18 633	27901	4 22 02.4	18 55 41	5.97	0.37	F4	47.3	5.06
vB 140	+04 686	279355	4 22 04.4	04 35 09	8.93	0.76	G5	49.5	7.09
vB 175	+16 593		4 22 07.9	16 52 17	10.31	1.04	K4	57.4	7.81
vB 54	+21 641	27934	4 22 23.4	22 10 49	4.22	0.14	A7	48.3	3.86
vB 55	+21 643	27946	4 22 26.4	22 05 12	5.28	0.25	A7	45.5	4.65
vB 56	+17 719	27962	4 22 36.0	17 48 53	4.29	0.05	A2	45.1	4.14
vB 57	+15 621	27991	4 22 46.2	15 49 40	6.46	0.49	F7	49.5	5.26
vB 58	+18 636	27989	4 22 57.1	18 45 05	7.53	0.68	G5	44.5	5.88
vB 59	+15 624	28034	4 23 14.9	15 24 43	7.48	0.54	G0	46.2	6.17
vB 60	+22 696	28024	4 23 19.0	22 42 04	4.28	0.26	A8	46.7	3.63
vB 62	+21 644	28033	4 23 20.7	21 21 28	7.38	0.54	F8	49.3	6.07
vB 141	+15 625	28052	4 23 30.0	15 30 22	4.49	0.25	F0	44.4	3.86
vB 68	+14 702	28258	4 23 32	14 37 51	5.89	0.32	G5	46.7	5.10
vB 63	+16 598	28294	4 23 32.3	16 44 28	8.03	0.65		45.0	6.45
vB 64	+16 601	28068	4 23 47.9	16 38 07	8.10	0.67	G1	45.0	6.48
Lei 59	+10 576	28099	4 24 02.7	10 45 33	9.46	1.03	G2	47.4	6.98
Lei 49		286820	4 24 06.3	13 01 36	10.46	1.14	K5	53.8	7.72
vB 177	+13 684		4 24 36.0	14 08 59	10.30	1.09	K7	46.4	7.68
vB 65	+15 627		4 24 45.0	15 28 42	7.42	0.54	K2	44.9	6.11
Lei 52		28205	4 24 57.5	14 18 25	9.49	0.93	G0	48.9	7.25
vB 66	+11 614		4 24 59.5	11 37 33	7.51	0.55		46.8	6.17
vB 67	+21 647	28237	4 25 02.8	21 30 35	5.72	0.27	F8	49.8	5.05
Lei 57	+18 639	28226	4 25 04.7	18 23 23	10.14	1.07	A m	48.9	7.57
Lei 50	+13 685		4 25 15.5	13 45 27	9.02	0.84	K2	50.9	6.99
vB 69	+19 727	28291	4 25 41.4	19 37 52	8.63	0.75	G5	49.7	6.82
vB 70	+18 640	28305	4 25 41.9	19 04 14	3.54	1.02	G9.5 III	45.7	1.08
vB 71	+15 631	28307	4 25 43.2	15 51 08	3.84	0.95	K0 IIIb	46.2	1.55
vB 72	+15 632	28319	4 25 48.5	15 45 40	3.40	0.18	A7 III	45.7	2.94
vB 73	+16 606	28344	4 25 55.4	17 10 34	7.85	0.60	G2	43.9	6.39
vB 74	+12 598	28355	4 26 02.2	12 56 17	5.02	0.22	A7	46.9	4.47
vB 75	+15 633	28363	4 26 08.2	16 02 58	6.59	0.63	F8	50.2	5.06
vB 76	+26 722	283704	4 26 26.1	26 33 46	9.19	0.76	G5	54.5	7.35
vB 77	+17 731	28394	4 26 27.3	17 26 09	7.04	0.50	G0	45.6	5.82
vB 78	+17 732	28406	4 26 36.8	17 45 16	6.91	0.45	F8	45.7	5.81
vB 79	+17 734	285773	4 26 37.9	17 47 04	8.96	0.83	G5	45.5	6.96
Lei 55			4 26 39.3	16 08 10	10.32	1.15		57.1	7.56
Lei 56	+16 609	28462	4 27 05.5	16 33 53	9.10	0.86	K1	47.6	7.02
vB 81	+19 731	28483	4 27 22.0	19 43 57	7.10	0.47	F5	50.9	5.95

TABLE 1. (continued)

Object	BD	HD	$\alpha(1950)^a$	$\delta(1950)^a$	V^b	B-V ^b	Sp. Ty. ^a	D(pc) ^c	K^d
vB 82	+15 637	28527	4 27 42.0	16 05 11	4.78	0.17	A6	46.5	4.34
vB182	+15 638	28545	4 27 43.7	15 37 36	8.94	0.85	K0	51.5	6.89
vB 83	+15 639	28546	4 27 47.8	15 35 03	5.48	0.26	A m	46.9	4.83
vB 84	+13 690	28556	4 27 48.5	13 36 60	5.41	0.26	F0	44.0	4.76
vB 85	+15 640	28568	4 27 55.1	16 02 29	6.51	0.43	F2	47.0	5.46
vB 86	+10 588	28608	4 28 11.6	10 38 40	7.04	0.47	F5	52.6	5.89
vB 87	+19 733	28593	4 28 19.3	20 01 35	8.59	0.74	G5	48.6	6.80
Lei 63	+17 744		4 28 43.6	17 36 13	9.55	0.98		43.5	7.19
vB 89	+15 645	28677	4 29 00.5	15 44 44	6.02	0.34	F4	46.0	5.18
vB 90	+05 674	28736	4 29 55.0	05 17 59	6.38	0.41	F5	41.8	5.37
vB 91	+15 646	28783	4 29 58.6	15 54 03	8.94	0.88	K0	51.2	6.82
vB 92	+15 647	28805	4 30 08.1	15 42 50	8.65	0.74	G5	51.7	6.86
vB 93	+16 620	28878	4 30 45.5	16 39 30	9.41	0.89	G5	57.4	7.26
vB 94	+12 608	28911	4 30 58.3	13 08 52	6.62	0.43	F2	50.1	5.57
vB 95	+14 720	28910	4 31 00.8	14 44 26	4.65	0.25	A8	45.7	4.02
vB 96	+14 721	285931	4 31 07.9	15 03 36	8.49	0.84	K1	48.4	6.46
vB 183	+15 650	28977	4 31 40.8	15 43 29	9.67	0.92	K0	59.5	7.45
vB 97	+15 651	28992	4 31 44.3	15 24 06	7.89	0.64	F8	49.7	6.34
vB 99	+15 654	29159	4 33 14.0	15 34 57	9.38	0.86	K0	54.1	7.30
vB 100	+23 715	29169	4 33 28.6	23 14 23	6.05	0.39	F5	44.7	5.09
vB 101	+15 656	29225	4 33 49.2	15 46 08	6.65	0.44	F8	52.1	5.57
vB 210	+11 633	286900	4 33 54.2	11 48 42	9.20	1.20	K2	30.3	6.32
vB 102	+14 728	29310	4 34 41.4	15 02 49	7.54	0.61	G0	43.2	6.06
vB 103	+15 661	29375	4 35 17.7	15 56 03	5.79	0.31	F0	50.3	5.02
vB 104	+12 618	29388	4 35 21.9	12 24 42	4.27	0.13	A6	44.4	3.93
Lei 83			4 35 31.4	17 26 38	10.18	1.15		48.9	7.42
vB 105	+22 721	29419	4 35 50.9	23 03 05	7.53	0.58	F5	43.4	6.12
vB 106	+13 702	29461	4 36 07.7	14 00 27	7.96	0.66	G5	47.0	6.36
vB 107	+07 681	29499	4 36 23.8	07 46 24	5.39	0.26	A5 m	48.1	4.74
vB 108	+15 666	29488	4 36 24.9	15 49 13	4.69	0.15	A5	55.3	4.30
+12 623		286929	4 37 03.0	12 37 53	10.04	1.08	K5	45.4	7.44
vB 109	+23 722	284574	4 37 05.1	23 12 28	9.40	0.81	K0	68.7	7.44
vB 185	+16 640	29608	4 37 33.1	16 25 03	9.47	1.10	K0	49.8	
Lei 90			4 40 22.5	16 58 34	9.85	1.00		55.8	7.44
vB 111	+10 621	30034	4 41 39.7	11 03 16	5.40	0.25	F0	44.9	4.77
vB 112	+11 646	30210	4 43 15.0	11 36 55	5.37	0.19	A m	63.8	4.89
vB 142	+15 678	30246	4 43 39.1	15 22 57	8.32	0.67	G5	48.6	6.70
Lei 92		30264	4 43 55.4	17 39 34	9.58	0.97		47.3	7.24
vB 113	+08 759	30311	4 44 01.6	08 55 42	7.26	0.56	F5	39.8	5.90
vB 114	+17 786	30355	4 44 42.8	18 10 15	8.53	0.72	G0	47.3	6.79
vB 115	+20 823	284787	4 45 43.8	21 00 51	9.07	0.84	G5	48.8	7.04
vB 116	+18 736	30505	4 46 08.3	18 33 17	8.99	0.83	F5	44.9	6.99
vB 117	+24 692	283882	4 46 09.9	24 42 59	9.59	1.05	K3	46.6	7.06
vB 118	+15 686	30589	4 46 40.2	15 48 10	7.74	0.58	F8	48.5	6.33
vB 119	+16 657	30676	4 47 30.4	17 07 05	7.11	0.56	F8	42.7	5.75
vB 120	+14 770	30712	4 47 42.8	14 59 55	7.59	0.73	G5	50.8	5.82
vB 121	+15 692	30738	4 47 56.3	16 07 34	7.29	0.50	F8	50.2	6.07
vB 122	+10 654	30810	4 48 26.3	10 59 02	6.77	0.53	F6	50.3	5.48
vB 123	+18 743	30780	4 48 27.0	18 45 22	5.11	0.21	A7	51.3	4.58
vB 143	+15 415	30809	4 48 31.8	15 20 58	7.89	0.53	F8	65.1	6.60
vB 124	+13 728	30869	4 49 00.7	13 34 18	6.27	0.50	F5	52.4	5.05
Lei 98	+27 667		4 49 28.0	18 54 53	10.29	1.07	F5	59.8	7.72

TABLE 1. (continued)

Object	BD	HD	$\alpha(1950)^a$	$\delta(1950)^a$	V^b	B-V ^b	Sp. Ty. ^a	D(pc) ^c	K ^d
vB 126	+19 811	31236	4 52 01.9	19 24 20	6.37	0.29	F3	57.8	5.65
vB 127	+13 749	31609	4 54 59.7	13 55 33	8.89	0.74	G5	59.8	7.10
vB 128	+15 713	31845	4 56 52.2	15 50 33	6.75	0.45	F5	44.5	5.65
vB 129	+21 751	32301	5 00 06.5	21 31 11	4.64	0.15	A7	55.3	4.25
Lei 107		32347	5 00 18.1	13 39 38	9.00	0.76		59.1	7.16
vB 151	+06 829	240629	5 02 59.3	06 23 52	9.92	0.95	K2	52.6	7.63
vB 215	+17 841	240648	5 03 23.3	17 45 01	8.82	0.73	K0	61.1	7.05
vB 202	+28 751		5 03 49.9	28 05 23	9.90	1.10	K0	43.5	7.25
vB 130	+09 743	33254	5 06 34.7	09 45 60	5.42	0.25	A2 m	53.6	4.79
vB 131	+27 732 B	33204	5 06 36.7	27 58 05	6.01	0.27	A5 m	58.1	5.34
vB 132	+27 732		5 06 36.7	27 58 05	8.59	0.69	A3	69.6	6.92

Notes to Table 1.

^a - from SIMBAD, ^b - Reid 1993 appendix, measurements from either Mermilliod 1976 or Pels et al. 1975^c - scaled value (see text) from Schwan 1991 or from Reid 1993 appendix, measurement from Pels et al. 1975^d - derived from B and B-V (see text)

TABLE 2. Summary of Observational Setups

	1993 Nov. 28-30	1994 Dec. 21-23	1995 Nov. 13-15	1996 Jan. 9-10
Number of Observations	24	54	68	47
pixel scale (arcsec/pixel) ^a	0.0385 ±0.0008	0.0352 ±0.0007	0.0326 ±0.0009	0.0326 ±0.0009
array	58x62 InSb	64x64 InSb subarray	64x64 InSb subarray	64x64 InSb subarray
rms readnoise (e ⁻)	450	80	80	80

Notes to Table 2.

^a - from Ghez et al. 1995 and similar observations of known binaries

TABLE 3. Hyades Speckle Binaries

Object	Date (UT)	ΔK (mag)	Separation (arcsec)	Position Angle (deg)	M_1 (M_\odot)	M_2 (M_\odot)	Comp.	Notes on ^d Binaries	Triples
vB 96	1995 Nov 13	0.70 ± 0.02^c	0.048 ± 0.001	288 ± 4	0.85	0.66	1	M: $0''192$, G: ~ 5000 dy	
+10 568	1996 Dec 23 ^b	0.70 ± 0.02	0.092 ± 0.002	330 ± 1					
	1996 Jan 09	0.14 ± 0.02^c	0.043 ± 0.001	213 ± 1	0.59	0.56	1	new	
	1997 Dec 14 ^b	0.14 ± 0.2	0.0463 ± 0.001	154 ± 1					
vB 91	1994 Dec 22	1.02 ± 0.02^c	0.058 ± 0.001	339 ± 10	0.81	0.56	1	M: $0''192$, G: >6000 dy	
	1996 Dec 22 ^b	1.02 ± 0.02	0.115 ± 0.002	340 ± 1					
vB 120	1996 Jan 10	0.25 ± 0.03	0.069 ± 0.002	31 ± 1	1.05	0.96	1	M: $0''082$, B&S: ?	
Lei 90	1994 Dec 22	2.35 ± 0.07	0.084 ± 0.003	12 ± 3	0.75	0.32	1	G: 3942dy	
vB 57	1993 Nov 28	0.58 ± 0.03	0.086 ± 0.002	289 ± 1	1.32	1.07	1	M: $0''099$, G: 2192dy, IDS: $0''1$	
vB 113	1995 Nov 15	2.7 ± 0.4	0.098 ± 0.002	124 ± 1	1.02	0.38	1	G: 2557dy	
vB 81	1996 Jan 10	2.13 ± 0.06	0.107 ± 0.002	114 ± 5	1.20	0.55	1	B&S: ?	
vB 24	1993 Nov 30	2.3 ± 0.4	0.139 ± 0.008	166 ± 6	1.80	1.00	1	M: $0''096$, S&L: 4177dy	
	1996 Jan 10	1.6 ± 0.1	0.146 ± 0.003	192 ± 2					
Lei 59	1996 Jan 09	$0.64 \pm .03$	0.137 ± 0.003	65 ± 1	0.69	0.54	1	new	
vB 103	1996 Jan 09	2.5 ± 0.2	0.158 ± 0.008	220 ± 1	1.70	0.68	1	new	
vB 114	1994 Dec 21	3.9 ± 0.1	0.17 ± 0.02	108 ± 3	0.87	0.21	1	G: >1826 dy	
vB 50	1993 Nov 28	1.39 ± 0.06	0.171 ± 0.005	180 ± 1	0.95	0.57	1	M: $0''262$, B&S: ?	
vB 59	1994 Dec 21	3.6 ± 0.2	0.184 ± 0.006	79 ± 2	1.07	0.28	1	G: >2557 dy	
vB 58	1994 Dec 21	0.60 ± 0.01	0.185 ± 0.004	162 ± 1	0.97	0.78	1	S&L: 10077dy, ADS: $0''34$	
Lei 20	1995 Nov 13	1.04 ± 0.04	0.202 ± 0.005	191 ± 1	0.72	0.49	2	new	G&G81: 2dy
Lei 83	1994 Dec 22	2.2 ± 0.04	0.212 ± 0.006	98 ± 3	0.68	0.30	2	new	G85: 61dy
vB 102	1996 Jan 09	2.0 ± 0.1	0.232 ± 0.005	280 ± 1	1.00	0.49	2	M: $0''235$	G: 731dy
vB 85	1995 Nov 13	3.0 ± 0.2	0.252 ± 0.006	63 ± 1	1.39	0.46	1	new	
vB 122	1995 Nov 15	0.0 ± 0.1	0.254 ± 0.006	142 ± 1	1.13	1.13	1	M: $0''209$, ADS: $0''13$, S&L: 5947dy	
vB 75	1993 Nov 28	0.9 ± 0.2	0.305 ± 0.008	103 ± 1	1.49	1.09	1	M: $0''411$, S&L: 14584dy, ADS: $0''11$	
Lei 92	1994 Dec 22	1.72 ± 0.01	0.310 ± 0.006	87 ± 1	0.69	0.37	1	new	
vB 29	1995 Nov 14	0.90 ± 0.02	0.321 ± 0.007	75 ± 1	1.17	0.84	1	ADS: $0''33$, S&L: 32595dy	
vB 185	1994 Dec 22	1.11 ± 0.01	0.443 ± 0.009	359 ± 1	0.80	0.53	2	M: $0''659$	G85: 277dy
vB 124	1995 Nov 15	1.3 ± 0.2	0.46 ± 0.01	153 ± 1	1.61	1.01	2	M: $0''452$, ADS: $0''1$, S&L: 34786dy	G85: 143dy
vB 17	1994 Dec 21	3.9 ± 0.3	0.73 ± 0.02	355 ± 1	0.85	0.21	1	new	
vB 151	1996 Jan 09	1.45 ± 0.06	0.85 ± 0.02	312 ± 1	0.64	0.37	2	new	G: 731dy
vB 5 ^a	1994 Dec 22	2.31 ± 0.05	0.88 ± 0.02	85 ± 1	0.68	0.29	1	new	
Lei 52 ^a	1995 Nov 13	5.5 ± 0.4	0.91 ± 0.02	15 ± 1	0.76	0.10	1	new	
Lei 130 ^a	1995 Nov 15	1.2 ± 0.1	0.99 ± 0.02	128 ± 1	0.58	0.38	1	new	
vB 52 ^a	1996 Jan 10	2.50 ± 0.07	1.02 ± 0.02	149 ± 1	0.91	0.36	1	B&S: ?	
+22 669 ^a	1995 Nov 13	2.9 ± 0.1	1.02 ± 0.02	208 ± 2	0.89	0.31	2	new	G82: 2dy
vB 40 ^a	1993 Nov 28	2.9 ± 0.5	1.33 ± 0.04	193 ± 1	1.15	0.39	2	ADS: $1''16$	G,S: 4dy

Notes to Table 3.

^a - Binary parameters determined from shift and add analysis^b - Keck measurement, ^c - Fixed to Keck flux ratio value^d - M - Mason et al. 1993, G - Griffin et al. 1988, B&S - Barrado y Navascues & Stauffer 1997, period unlisted, counted as binary not triple (see text)

IDS - IDS catalogue, S&L - Stefanik & Latham 1992, ADS - ADS catalogue, G&G81 - Griffin & Gunn 1981, G85 - Griffin et al. 1985

G82 - Griffin et al. 1982, G,S - Sanford 1921, listed in Griffin et al. 1988

TABLE 4. Limits for Undetected Companions to Hyades Speckle Singles

Object	Date (UT)	ΔK_{lim}	$M(M_{\odot})$	$M_{lim}(M_{\odot})$	# Comp.	Notes on Other Measurements ^a
+20 480	1996 Jan 09	3.69	1.36	0.35	0	
vB 1	1995 Nov 14	4.46	1.05	0.20	0	
Lei 2	1995 Nov 14	4.29	0.62	0.13	0	
+35 714	1994 Dec 21	4.48	1.19	0.23	1	M: 0''222
vB 4	1994 Dec 22	3.76	0.78	0.19	0	
+16 516	1995 Nov 13	3.20	0.83	0.26	1	N&Y: 0.5dy(WD)
vB 170	1995 Nov 15	4.03	0.61	0.14	0	
vB 6	1993 Nov 28	3.73	1.49	0.38	0	
vB 7	1995 Nov 13	3.86	0.79	0.19	0	
vB 8	1996 Jan 10	2.87	1.36	0.47	0	
Lei 11	1995 Nov 13	3.25	0.63	0.19	0	
Lei 10	1994 Dec 22	3.54	0.80	0.22	0	
vB 10	1996 Jan 10	4.16	0.99	0.22	0	
Lei 15	1996 Jan 10	4.50	0.66	0.13	0	
Lei 16	1995 Nov 13	3.54	0.64	0.17	0	
vB 11	1993 Nov 28	3.01	1.47	0.49	1	ADS: 2''0
+13 647	1994 Dec 21	3.98	1.12	0.26	0	
Lei 18	1995 Nov 13	3.66	0.80	0.21	0	
+8 642	1995 Nov 15	3.86	0.72	0.17	0	
vB 13	1994 Dec 21	4.76	1.32	0.23	0	
vB 14	1996 Jan 10	3.25	1.47	0.45	1	B&S: ?
vB 16	1996 Jan 10	3.73	1.36	0.35	0	
vB 15	1994 Dec 21	3.62	0.91	0.24	0	
vB 18	1994 Dec 21	4.08	0.96	0.22	0	
vB 19	1995 Nov 15	3.80	1.18	0.29	0	
vB 162	1996 Jan 10	2.87	1.12	0.39	1	G&G81: 55dy
vB 20	1995 Nov 15	4.03	1.48	0.34	0	
vB 21	1995 Nov 13	3.62	0.78	0.21	0	
vB 22	1994 Dec 21	4.43	1.01	0.20	1	G85: 6dy
vB 23	1996 Jan 10	4.01	1.23	0.28	1	B&S: ?
vB 25	1994 Dec 21	4.25	0.70	0.15	0	
vB 26	1996 Jan 10	4.11	0.85	0.19	0	
vB 27	1995 Nov 15	3.73	0.93	0.24	0	
vB 28	1996 Jan 09	1.04	giant	4.38	0	
vB 30	1995 Nov 14	3.25	1.66	0.50	0	
vB 31	1995 Nov 15	4.35	1.09	0.22	0	
vB 32	1996 Jan 10	3.08	1.51	0.49	0	
vB 33	1996 Jan 10	3.73	1.89	0.48	0	
vB 34	1993 Nov 28	3.89	1.70	0.41	2	S&L: 3dy, BV: ?(WD)
vB 35	1993 Nov 28	4.08	1.34	0.30	0	
vB 36	1993 Nov 28	3.01	1.29	0.43	0	
vB 37	1994 Dec 21	4.48	1.36	0.26	0	
vB 38	1995 Nov 14	3.58	1.68	0.45	1	S&L: 2dy
vB 39	1996 Jan 10	2.70	0.89	0.33	1	G: >2557dy
vB 41	1996 Jan 09	4.58	giant	1.19	2	M: 0''273, G: 530dy
vB 42	1996 Jan 09	4.53	0.85	0.16	0	
vB 43	1995 Nov 15	4.03	0.80	0.18	1	G85: 591dy
vB 44	1996 Jan 10	2.94	1.26	0.43	0	
vB 45	1995 Nov 14	3.80	1.78	0.44	1	S&L: 8dy
vB 46	1994 Dec 21	4.20	0.75	0.16	0	
vB 47	1996 Jan 09	4.20	2.09	0.45	0	
vB 48	1993 Nov 28	3.66	1.13	0.30	0	

TABLE 4. (continued)

Object	Date (UT)	ΔK_{lim}	$M(M_{\odot})$	$M_{lim}(M_{\odot})$	# Comp.	Notes on Other Measurements ^a
vB 49	1995 Nov 15	3.40	0.92	0.26	0	
vB 174	1995 Nov 15	4.20	0.73	0.16	0	
vB 51	1993 Nov 28	3.98	1.27	0.30	0	
vB 53	1995 Nov 14	3.95	1.65	0.39	0	
vB 140	1996 Jan 09	4.33	0.81	0.17	1	G85: 156dy
vB 175	1995 Nov 15	4.03	0.70	0.16	0	
vB 54	1994 Dec 23	4.52	2.61	0.50	0	
vB 55	1996 Jan 09	4.31	1.86	0.38	0	
vB 56	1996 Jan 09	4.31	2.23	0.46	0	
vB 60	1994 Dec 23	4.23	2.76	0.59	0	
vB 62	1995 Nov 14	3.54	1.18	0.32	1	G&G78: 9dy
vB 141	1996 Jan 09	3.66	2.44	0.64	1	A: 5200dy
vB 68	1996 Jan 10	4.18	1.61	0.35	0	
vB 63	1995 Nov 14	2.94	0.95	0.32	1	G: 2557dy
vB 64	1996 Jan 09	4.03	0.94	0.21	0	
Lei 49	1995 Nov 13	3.49	0.82	0.66	0	
vB 177	1994 Dec 21	4.31	0.62	0.13	0	
vB 65	1995 Nov 13	4.27	1.08	0.23	0	
vB 66	1995 Nov 14	4.48	1.09	0.21	0	
vB 67	1995 Nov 15	3.98	1.73	0.40	0	
Lei 57	1994 Dec 22	4.31	0.68	0.14	1	G85: 1907dy
Lei 50	1994 Dec 22	4.01	0.86	0.20	0	
vB 69	1995 Nov 14	3.01	0.90	0.30	1	G85: 42dy
vB 70	1996 Jan 09	4.5	giant	1.33	0	
vB 71	1996 Jan 09	4.63	giant	1.07	1	M: 0''048, G: 5844dy
vB 72	1994 Dec 23	4.01	evolved	0.80	1	S&L: 140dy
vB 73	1995 Nov 14	3.76	0.95	0.24	0	
vB 74	1994 Dec 23	5.10	2.04	0.31	0	
vB 76	1996 Jan 10	2.94	1.73	0.39	0	
vB 77	1995 Nov 14	3.31	0.80	0.27	1	G85: 239dy
vB 78	1996 Jan 10	3.01	1.22	0.40	0	
vB 79	1994 Dec 22	3.62	0.80	0.21	0	
Lei 55	1994 Dec 22	3.76	0.77	0.19	0	
Lei 56	1994 Dec 22	4.13	0.81	0.18	0	
vB 82	1994 Dec 23	4.76	2.12	0.37	0	
vB 182	1994 Dec 22	3.95	0.90	0.21	1	G&G81: 358dy
vB 83	1995 Nov 13	4.13	1.78	0.39	1	A&L: 106.3dy
vB 84	1995 Nov 13	3.83	1.74	0.43	0	
vB 86	1996 Jan 09	4.53	1.32	0.25	0	
vB 87	1996 Jan 09	4.55	0.89	0.17	0	
Lei 63	1994 Dec 22	3.76	0.71	0.18	1	G: 845dy
vB 89	1995 Nov 14	3.95	1.54	0.36	0	
vB 90	1996 Jan 09	4.31	1.33	0.27	0	
vB 92	1994 Dec 22	4.31	0.92	0.19	0	
vB 93	1994 Dec 22	4.11	0.86	0.19	0	
vB 94	1995 Nov 13	3.95	1.44	0.34	0	
vB 95	1994 Dec 23	4.53	2.35	0.45	1	A: 488.5dy
vB 183	1994 Dec 22	3.80	0.82	0.20	0	
vB 97	1995 Nov 13	4.45	1.07	0.21	0	
vB 99	1994 Dec 22	3.73	0.81	0.21	0	
vB 100	1995 Nov 15	3.20	1.56	0.48	0	
vB 101	1995 Nov 14	3.49	1.48	0.41	0	

TABLE 4. (continued)

Object	Date (UT)	ΔK_{lim}	$M(M_{\odot})$	$M_{lim}(M_{\odot})$	# Comp.	Notes on Other Measurements ^a
vB 210	1995 Nov 14	4.03	0.73	0.17	0	
vB 104	1994 Dec 23	4.82	2.38	0.4	0	
vB 105	1995 Nov 15	4.33	1.04	0.21	0	
vB 106	1995 Nov 14	4.20	1.02	0.22	1	G: 3653dy
vB 107	1996 Jan 09	4.23	1.88	0.40	0	
vB 108	1994 Dec 23	4.52	2.47	0.47	0	
+12 623	1994 Dec 22	4.08	0.67	0.15	0	
vB 109	1995 Nov 15	3.69	0.93	0.24	0	
vB 111	1996 Jan 09	4.39	1.76	0.35	0	
vB 112	1995 Nov 15	3.58	2.23	0.60	1	A&L: 18dy
vB 142	1994 Dec 22	4.60	0.93	0.17	1	B&S: ?
vB 115	1994 Dec 21	4.60	0.82	0.15	1	G: 1461dy
vB 116	1996 Jan 10	3.08	0.78	0.25	0	
vB 117	1995 Nov 15	4.35	0.78	0.16	1	G&G78: 12dy
vB 118	1994 Dec 22	3.89	1.06	0.25	0	
vB 119	1995 Nov 13	3.49	1.18	0.33	1	B&S: ?
vB 121	1995 Nov 13	4.48	1.20	0.23	1	G&G78: 6dy
vB 123	1995 Nov 14	3.76	2.10	0.53	0	
vB 143	1994 Dec 22	4.20	1.21	0.26	0	
Lei 98	1995 Nov 15	3.08	0.75	0.24	0	
vB 126	1995 Nov 14	3.36	1.56	0.46	0	
vB 127	1994 Dec 22	3.92	0.94	0.22	0	
vB 128	1996 Jan 09	4.01	1.27	0.29	0	
vB 129	1995 Nov 14	3.69	2.51	0.65	0	
Lei 107	1995 Nov 15	3.36	0.91	0.27	0	
vB 215	1995 Nov 15	3.80	0.97	0.24	0	
vB 202	1996 Jan 10	3.08	0.69	0.22	0	
vB 130	1996 Jan 09	4.08	2.01	0.45	1	B&C: 155.8dy
vB 131	1996 Jan 10	3.92	1.76	0.42	1	S&L: 11725dy
vB 132	1994 Dec 21	3.08	1.13	0.37	1	M: 0''290, ADS: 0''31

Notes to Table 4.

^a - M - Mason et al. 1993, N&Y - Nelson & Young 1976, ADS - ADS catalogue

B&S - Barrado y Navascues & Stauffer 1997 (period unlisted), G&G81 - Griffin & Gunn 1981

G85 - Griffin et al. 1985, S&L - Stefanik & Latham 1992, BV - Bohm-Vitense 1993, G - Griffin et al. 1988

G&G78 - Griffin & Gunn 1978, A - Abt 1965, A&L - Abt & Levy 1985, B&C - Burkhart & Coupry 1989

TABLE 5. Field Star K-band Luminosity Function

M_K	mass (M_\odot)	p^a	N^b (Hyades)	$N(r < 3pc)$	$N(r > 3pc)$	N (A0-F6)	N (F7-G9)	N (K0-K5)
0.0		100	0	0	0	0	0	0
1.0	2.6	99.3	0	0	0	0	0	0
2.0	1.8	97.9	0	0	0	0	0	0
3.0	1.2	96.5	0	0	0	0	0	0
4.0	0.8	92.4	0	0	0	0	0	0
5.0	0.6	79.9	9	2	7	9	0	0
6.0	0.4	70.8	37	15	22	34	3	0
7.0	0.3	48.6	29	5	24	7	17	5
8.0	0.2	26.4	41	4	37	1	19	21
9.0	0.1	12.5	13	1	12	0	1	12
10.0	0.09	0.7	0	0	0	0	0	0
11.0	0.06	0	0	0	0	0	0	0
12.0	0.05	0	0	0	0	0	0	0
missing %			46	59	43	68	39	25

Notes to Table 5.

^a - the percentage of the field sample with fainter magnitudes

^b - the number of unresolved stars in the Hyades speckle sample with detection limits, M_{Klim} , from $(> M_K - 1)$ up to and including (M_K)

TABLE 6. Companion Star Fraction

Subsample	Targets	# Comp. ^a	5 ≤ Separation ≤ 50AU		All Separations	
			$csf_{5-50AU,obs}$	$csf_{5-50AU,corr}$	# Mult. ^b	$msf_{total,obs}$
MS stars	162	26	0.16 ± 0.03	0.30 ± 0.06	66	0.41 ± 0.05
r ≤ 3.0pc	33	5	0.15 ± 0.07	0.37 ± 0.17	14	0.42 ± 0.11
r > 3.0pc	129	21	0.16 ± 0.04	0.28 ± 0.07	52	0.40 ± 0.06
.05 < (B − V) < .47 (A0-F6)	55	4	0.07 ± 0.04	0.22 ± 0.19	15	0.27 ± 0.07
.49 < (B − V) < .76 (F7-G9)	55	12	0.22 ± 0.06	0.36 ± 0.10	30	0.55 ± 0.10
.81 < (B − V) < 1.20 (K0-K5)	52	10	0.19 ± 0.06	0.25 ± 0.08	21	0.40 ± 0.09

Notes to Table 6.

^a - IR Speckle binaries in the restricted separation range^b - Includes all speckle binaries and systems discovered by other techniques